



# Chip formation simulation and analysis of the mechanical loads during micro single-lip deep hole drilling of Inconel 718 with varying cooling lubricant pressure

Ekrem Oezkaya<sup>1</sup> · Sebastian Michel<sup>1</sup> · Dirk Biermann<sup>1</sup>

Received: 27 November 2020 / Accepted: 12 January 2021 / Published online: 6 February 2021  
© German Academic Society for Production Engineering (WGP) 2021

## Abstract

The micro single-lip deep hole drilling process is subjected to many difficulties. Especially the machining of difficult-to-cut materials like the nickel-based alloy Inconel 718 results in high thermal and mechanical loads. Irregularities in the drilling process, which lead to early tool failures must be avoided. A major challenge for micro single-lip deep hole drilling is to generate favorable chips and guarantee good chip removal. Since the chip flute of single-lip deep hole drilling tools is straight, the only mechanism to transport the chips and remove them from the bore hole is the coolant flow. In this paper the mechanical loads and the resulting chip formation for various cooling lubricant pressures are analyzed using tools with a diameter of  $d=2$  mm. In the experiments feed force, drilling torque, tool wear, bore hole quality as well as diameter and roundness deviations were evaluated. Individual chips are digitized and prepared as CAD models for the future consideration of the chip removal in flow simulations of the cooling lubricant. Additional FEM computational analyses of the three-dimensional chip formation with a geometric representation of the chip shape were carried out. This way not only provides valuable validated information about the process and the chip formation but also creates a basis for further investigations, which will allow an innovative simulation of the coolant flow and considers the chip formation and the chip shape.

**Keywords** Single-lip deep hole drilling · Chip formation · Chip shape · Inconel 718 · FEM simulation

## List of symbols

$A$	Yield stress, N/mm <sup>2</sup>
$B$	Strain hardening exponent
$C$	Dimensionless strain rate
$d$	Diameter, mm
$D$	Diameter deviation, $\mu\text{m}$
$F_f$	Feed force, N
$f$	Feed rate, mm
$h_c$	Heat transfer coefficient, W/m <sup>2</sup> ·K
$l$	Length, mm
$le$	Minimum element edge length, mm
$l_f$	Drilling path, mm
$l_t$	Drilling depth; mm
$m$	Exponent for the softening
$n$	Spindle speed, min <sup>-1</sup>
$nc$	Hardening coefficient
$p$	Pressure, bar

$P$	Spindle power, kW
$Ra$	Arithmetical mean roughness, $\mu\text{m}$
$Rz$	Ten-point mean roughness, $\mu\text{m}$
$T$	Temperature, K; torque, Nm
$T_K$	Roundness deviation
$t$	Time, s
$v_c$	Cutting speed, m/min

## Greek symbols

$\dot{\epsilon}$	Equivalent plastic strain rate, 1/s
$\epsilon_0$	Reference equivalent plastic strain rate, 1/s
$\kappa$	Angles of incidence, °
$\mu$	Viscosity, mm <sup>2</sup> /s
$\rho$	Density, g/cm <sup>3</sup>
$\sigma$	Equivalent stress, N/mm <sup>2</sup>

## Abbreviations

CAD	Computer-aided design
CFD	Computational fluid dynamics
FEM	Finite element method
SLD	Single-lip deep hole drill
STL	Standard triangulation language
VB	Wear mark width

✉ Ekrem Oezkaya  
ekrem.oezkaya@tu-dortmund.de

<sup>1</sup> Institute of Machining Technology, TU Dortmund University, Baroper Straße 303, 44227 Dortmund, Germany

## 1 Introduction

Deep hole drilling processes are widely used in many industrial applications, e.g. in the medical industry for biomedical products, for fuel injectors in the automotive industry or for cooling holes in turbine engines in the aerospace industry [1, 2]. Single-lip deep hole drills (SLD) are used in the diameter range of  $d=0.5\text{--}80$  mm and allow high length-to-diameter ratios up to  $l/d=900$  with very high hole qualities [3]. The cooling lubricant for the drilling process is delivered through one or more cooling channels which pass through the tool shank and removes the mixtures of chips and cooling lubricant along a flute or longitudinal groove (bead) at the outside of the tool shank [4]. An unfavorable chip formation leads to long chips, which may harm the surface quality of the bore hole. For higher drilling depths and longer process times the risk of chip jamming increases significantly. In combination with high mechanical and thermal loads tool failure therefore becomes more likely [5]. With small tool diameters the ratio of cutting edge radius and feed rate becomes greater than 1, which leads to negative effective rake angles resulting in high compressive stresses at the cutting edge [6]. Especially in micro deep hole drilling of difficult-to-cut materials there are many challenges such as large drilling forces, high temperatures, difficult chip removal, straightness deviations and a low rigidity of the tool leading to easy tool fracture, severe wear or low bore hole qualities [7]. The properties of nickel-based superalloys, especially of Inconel 718, are responsible for a poor machinability [8]. The high heat resistance of the material, the strong tendency to work hardening and the low heat dissipation lead to high thermo-mechanical loads of the tools and support abrasive and adhesive tool wear, which in turn influences the quality of the bore hole [9]. With standard cutting tip geometries the material properties also promote the formation of long and folded chips. These chips are difficult to remove from the bore hole and tend to jam in the chip flute, resulting in additional loads and higher temperatures, which can result in tool breakage [10]. Therefore, the chip formation and the chip removal are the main challenges in micro deep hole drilling [11, 12].

In the past, many analytical, numerical and experimental investigations of chip formation, chip flow and chip breaking were carried out [13–18]. Particularly for drilling it is important to move from 2D modeling to a 3D modeling of the processes to consider the complex geometries of the cutting engagement and enable the mapping of complex interactions such as the effects of cooling lubricants [15]. 3D analysis considers the tool geometry and the effects resulting from the tool rotation can

be simulated [19]. The current knowledge of the cooling lubricant behavior is very limited, so that new simulation models must be developed to optimize the drilling process and create innovative tool designs [15]. The mechanics of micro cutting differ fundamentally from conventional macro cutting and require quite different assumptions and need new modeling approaches concerning the underlying material behavior and the cutting engagement [20]. Therefore, in this paper a model as a basis for an expanded process simulation is established. To generate input data and to validate the simulation results experimental tests are carried out. The chip formation and the mechanical loads during micro single-lip deep hole drilling are investigated at various cooling lubricant pressures. The tool diameter is  $d=2$  mm and the workpiece material is Inconel 718. To create the basis for further investigations of the cooling lubricant supply, in which the chip formation and the chip removal can be considered, a finite element method (FEM) simulation with the software DEFORM 3D is carried out to generate a geometric representation of the chip shape. The FEM simulation of the chip formation is validated with the experimental data, i. e. the mechanical loads (feed force and drilling torque). Since a 3D FEM simulation of a complete chip from multiple rotations of the tool is not possible for economic reasons, a geometrical representation is generated using digital 3D scans of chips from the experiments. Together with the chip formation the chip shape can be positioned along the chip flute and integrated into the validated FEM model. This preliminary work forms the basis for the coupling of the results on chip shape and chip formation from the FEM simulation with a computational fluid dynamics simulation (CFD) of the cooling lubricant supply. This enables a detailed analysis of the interactions between the fluid / tool / workpiece / chip formation and chip shape. The behavior and effects of the cooling lubricant in interaction with various cutting parameters when drilling difficult-to-machine materials such as Inconel 718 are still not sufficiently understood today [21, 22]. The modelling of the chip formation and of the chip shape are necessary and important milestones, to carry out further analysis and to develop innovative methods for the optimization of micro single-lip deep hole drilling tools and processes.

## 2 Experimental set-up and results

The experimental analyses are carried out on a conventional deep hole drilling machine ML 200 from TBT. The tools are made of solid carbide and have a standard cutting tip geometry with angles of incidence of  $\kappa_1 = 50^\circ$  at the outer and  $\kappa_2 = 120^\circ$  at the inner cutting edge. The properties of the nickel-based alloy Inconel 718 and the cooling

**Table 1** Properties of Inconel 718

Chemical composition, %			
Ni	53.77	Si	0.08
Cr	17.92	Mn	0.06
Fe	Rest	V	0.06
Nb	5.42	Cu	0.04
Mo	2.88	W	0.02
Ti + Ta	< 1.0	P	0.011
Al	0.51	Zr	< 0.01
Co	0.21	B	0.004
Physical properties			
Type	SWISSCUT ORTHO NF-X 10		
Density at $T=20\text{ }^{\circ}\text{C}$	$\rho = 0.857\text{ g/cm}^3$		
Middle-point viscosity	$\mu = 10.4\text{ mm}^2/\text{s}$ (40 °C)		
Flash point at $p=1013\text{ mbar}$	$T = 155\text{ }^{\circ}\text{C}$		
Ignition temperature at $p=1013\text{ mbar}$	$T = > 240\text{ }^{\circ}\text{C}$		
Steam pressure at $T=20\text{ }^{\circ}\text{C}$	$p = < 3\text{ mbar}$		

lubricant, type Swisscut Ortho NF-X 10 from Motorex are listed in Table 1. During preliminary tests, a cutting speed of  $v_c = 30\text{ m/min}$  and a feed rate of  $f = 0.008\text{ mm}$  for a stable single-lip deep hole drilling process using small diameter single-lip drilling tools of  $d = 2\text{ mm}$  could be determined. The analysis of the process was carried out with varying cooling lubricant pressures in the range of  $p = 80\text{ bar}$  to  $p = 120\text{ bar}$ . In addition to mechanical tool loads, tool wear and chip shapes, the bore hole quality in form of surface roughness as well as diameter and roundness deviations were evaluated.

The mechanical loads were measured with a piezoelectric dynamometer type 9272 and a charge amplifier type 5011B from Kistler and were evaluated with the software Labview. At the beginning of the drilling process, the single-lip deep hole drill was guided in a pilot hole in order to avoid influencing the measurement of the mechanical load due to the force shunt by placing a drill bush on the workpiece. The chip shapes and the tool wear are analyzed with a Keyence VHX-5000 digital microscope. The analysis of the bore hole quality was carried out with a PRISMO 5 HTG VAST 3D measuring machine from Zeiss. The investigation of the

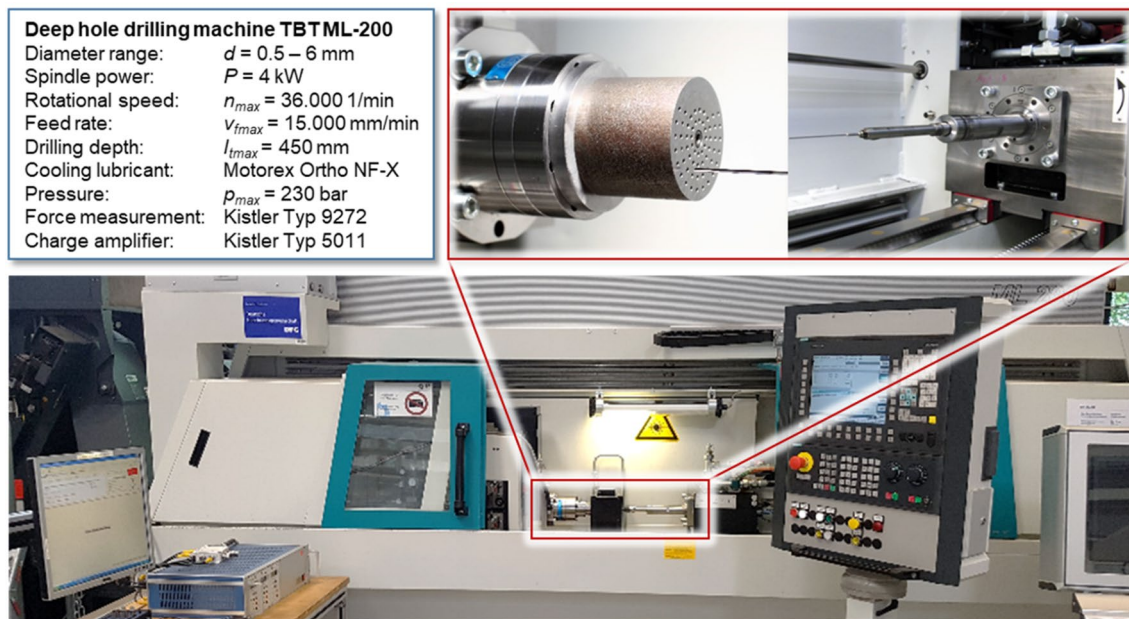


**Fig. 1** Experimental set-up

surface quality is carried out tactile with a roughness measuring machine Mahr MarSurf XR20. The experimental setup and the technical properties of the drilling machine are shown in Fig. 1.

## 2.1 Mechanical loads and chip shapes

To generate a database for the validation of the FEM simulation model of the chip formation, the mechanical loads were measured. The tools were analyzed over a total drilling path of  $l_f=1440$  mm. The mechanical loads in the form of feed force and drilling torque were evaluated at a total drilling path of  $l_t=48$  mm. This avoids the risk of large deviations between the measurements due to the rapidly changing initial tool wear. For statistical validation of the results, the tests were repeated under identical conditions. The results show a stable drilling process with very low deviations for the measurements of the feed forces and the drilling torques. When analyzing the results, it initially appears that the increase in feed force with higher cooling lubricant pressures results from the effect of the pressure of the lubricant on the bottom of the bore hole (Fig. 2). The measurement of the feed forces and torques was started after threading the tool into the bore hole and after switching on the cooling lubricant supply. Therefore the pressure of the coolant at the bore hole bottom has no influence on the measurement. The increase of the feed force with increasing coolant pressure therefore results from the better cooling effect in the contact zone and the resulting lower thermal softening of the material.

Regarding the drilling torque, no significant influence of the cooling lubricant pressure can be determined. While there is a slight increase in the drilling torque between  $p=80$  bar and  $p=100$  bar, the drilling torque drops slightly again at a pressure of  $p=120$  bar. The high cooling lubricant pressure suggests an improvement in chip removal, which leads to less friction between the bore hole wall and the

chips transported in the chip flute. The minor deviations of the drilling torque between the tests correlate with the analysis of the chip shapes (Fig. 3). Throughout the entire wear process it can be observed for all used coolant pressures, that relatively long slightly coiled and folded chips are produced. Compared to short spiral chips, these chip shapes make chip evacuation more difficult. If the chips get jammed between the tool and the workpiece, a chip jam occurs, which increases the risk of tool breakage, especially with high drilling depths and long tools. The chips for the cooling lubricant pressures  $p=100$  bar and  $p=120$  bar are slightly shorter than the chips at a pressure of  $p=80$  bar. Due to the higher cooling lubricant pressure, higher forces act on the chip during chip formation, which promote chip breakage.

## 2.2 Tool wear and bore hole quality

The tool wear determined in the experimental tests is evaluated by measuring the wear mark width  $VB$  (Fig. 4). The maximum width of the wear mark  $VB$  on the flank face before stopping the experiments was set to  $VB=100$   $\mu\text{m}$  and was reached for all coolant pressures after a drilling path of approx.  $l_f=1440$  mm. Up to a drilling path of about  $l_f=144$  mm the tools show a steeper increase in  $VB$ , which represents the initial wear of the tools. After the drilling path of  $l_f=144$  mm the tool wear progresses slowly for all tools. The curves for the wear mark width in Fig. 4 represent in each case for  $p=80$  bar,  $p=100$  bar and  $p=120$  bar an averaged value of the tests carried out under identical conditions. Corresponding to the measurement of the mechanical loads the results showed only minimal deviations. For a coolant pressure of  $p=80$  bar and  $p=100$  bar the development of tool wear over the drilling path is comparable. Due to the better heat removal at higher coolant pressures the tools show lower wear for a coolant pressure of  $p=120$  bar. Regarding the bore hole quality, the tests with a cooling

**Fig. 2** Comparison of the mechanical loads (feed force and drilling torque) for various coolant lubricant pressures

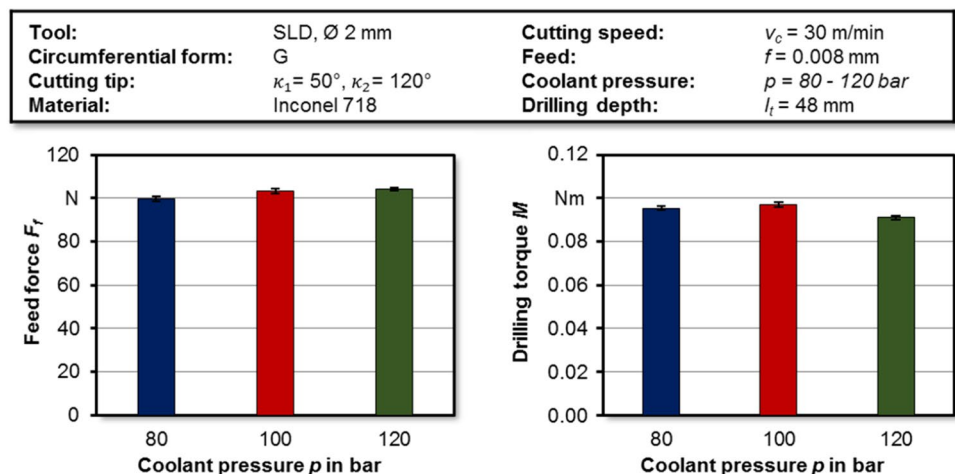


**Fig. 3** Analysis of chip shape depending on coolant lubricant pressure

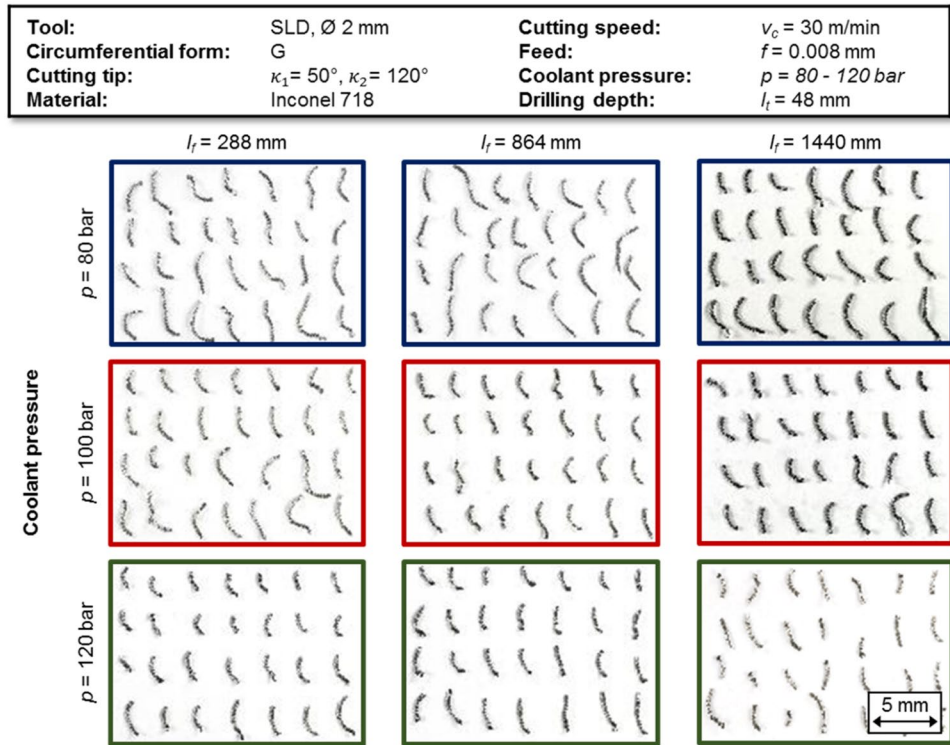
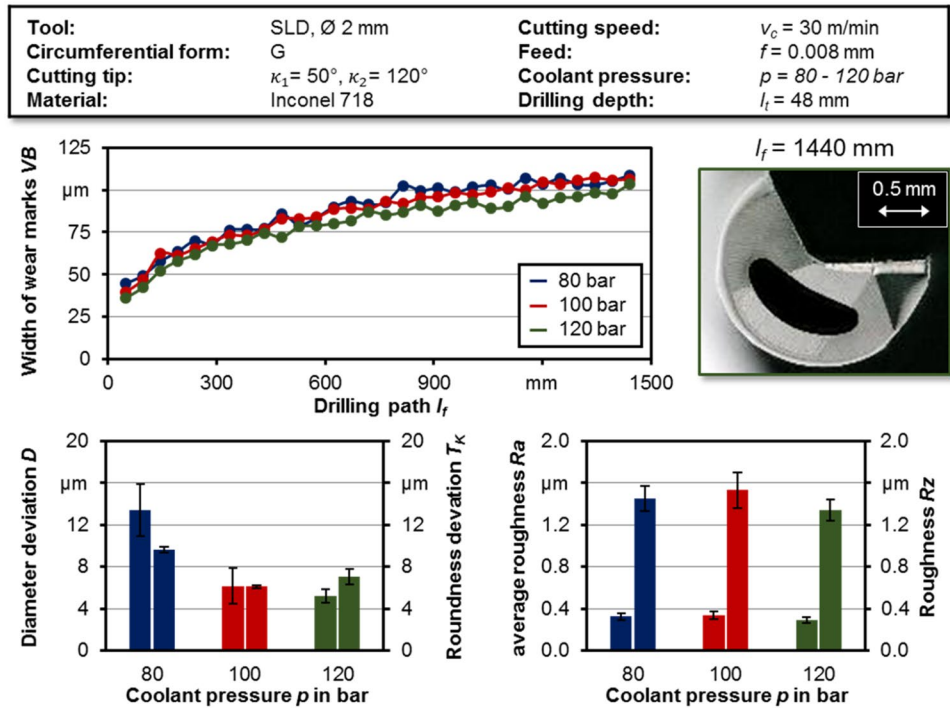


**Fig. 4** Analysis of tool wear and bore hole quality at various coolant lubricant pressures



lubricant pressure of  $p = 120$  bar also show good results. However, the differences between the results for varying coolant pressures in terms of surface quality ( $Ra$  and  $Rz$ ) are relatively small. The roughness is typically strongly dependent on the feed rate, which was kept constant during the

experiments. Only the diameter and roundness deviations for the tests with a coolant lubricant pressure of  $p = 80$  bar show higher values and bigger deviations. This again indicates an influence of higher temperatures due to the lower coolant pressure in the contact zone between tool and workpiece.

The drilling process with a cutting speed of  $v_c = 30$  m/min and a feed rate of  $f = 0.008$  mm turns out to be very stable overall and forms a good basis for the generation of valid measurement data for the generation and validation of suitable simulation models for the holistic representation of the drilling process, taking into account tool geometry, chip formation, chip removal and coolant supply. With regard to the cooling lubricant pressures, only slight differences between the selected pressure levels can be detected. Due to the slightly increased diameter deviations at a pressure of  $p = 80$  bar, a cooling lubricant pressure of  $p = 100$  bar will be selected for further consideration of the process in future investigations to map the cooling lubricant supply within the framework of a CFD simulation.

### 3 FEM computational analyses

The three-dimensional geometry for the simulation of the micro single-lip deep hole drilling process contains several components (bore hole wall, tool and bore hole bottom) and was designed with the computer-aided design (CAD) software SolidWorks. After correctly positioning the components in relation to one another the assembly has been transferred into the Software DEFORM 3D (Fig. 5). For the FEM simulation of the chip formation, the length of

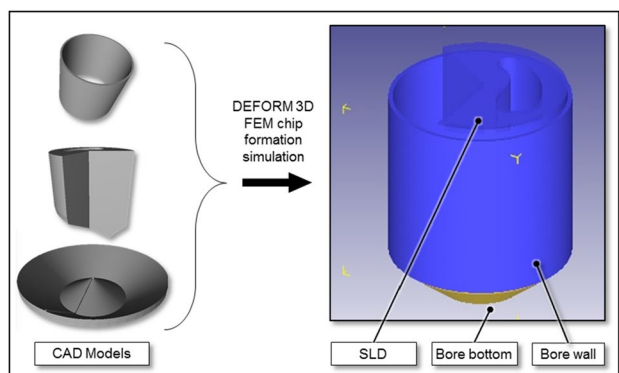


**Fig. 5** CAD model with positioned components for the transfer into DEFORM 3D

the SDL was reduced to a length of  $l = 2.5$  mm and the bore hole bottom to a length of  $l = 0.1$  mm. The bore hole wall with a length of  $l = 2$  mm is fixed on the workpiece. Due to the contact between bore hole wall and the developing chip, the bore hole wall plays an important role for a realistic representation of the whole chip formation. Since the contact between the chip and the bore hole wall is limited, the computational performance is hardly affected. The model is meshed with 3D tetrahedral elements. The mesh density of the bore hole bottom (workpiece) was increased since the chip formation taking place in this area leads to high gradients of plastic strain. The tool and the bore hole wall are modeled as rigid and have a constant mesh, which is finer at the cutting edge. In the contact zone the mesh elements are stretched and severely distorted during the simulation. Convergence problems can be minimized by regularly adapting and mapping the mesh and the corresponding solutions of the stretched and severely distorted mesh elements in the contact zone to a new mesh. The relationship of accuracy and required computing power for the mesh density is an important topic. In many instances the minimum number of elements is set by topological considerations [23]. The meshing of complex and small machining tools such as the micro SDL is a particular challenge since the cutting engagement differs with low feed rates and changing effective rake angles. In the already very small cutting zone the minimum element edge length must be at least three times smaller than the uncut chip thickness [24]. The minimum element edge length of  $le = f/3$  with a feed rate of  $f = 0.008$  mm results in a value of  $le = 0.0027$  mm in the simulation. Therefore the meshing is a highly demanding task. Since the preparation of the model already considers the cutting engagement with a geometrical imprint of the tool on the bore hole bottom, the cutting edge has full contact at the beginning of the simulation. The boundary conditions for the FEM chip simulation are listed in Table 2.

In order to describe the complex material flow behavior of Inconel 718 and accurately model the material behavior in the shear zone, the material model from Johnson & Cook was used [25]. The Johnson & Cook model describes the flow stress considering the material strain, strain rate and

**Table 2** Boundary conditions for the FEM chip simulation

Tool		Workpiece	
Tool Geometry	$\kappa_1 = 50^\circ, \kappa_2 = 120^\circ$	Material	Inconel 718
Diameter	$d = 2$ mm	Material model	Johnson and Cook
Feed rate	$f = 0.008$ mm	Friction; hybrid	Shear = 0.45 Columb = 0.5
Simulation time	$t = 0.0016$ s	Heat transfer coefficient	$h_c = 45$ W/m <sup>2</sup> •K
Elements	150,000	Elements	350,000
Object type	rigid	Object type	plastic

the thermal influence. The equivalent stress  $\sigma$  can be calculated with:

$$\sigma = (A + B\epsilon^{nc}) \left[ 1 + C \ln \left( \frac{\dot{\epsilon}}{\dot{\epsilon}_0} \right) \right] \left[ 1 - \left( \frac{T - T_r}{T_m - T_r} \right)^m \right] \quad (1)$$

whereby,  $A$ ,  $B$ ,  $C$ ,  $nc$  and  $m$  are the material parameters,  $\dot{\epsilon}$  is the equivalent plastic strain rate,  $\dot{\epsilon}_0$  the reference equivalent plastic strain rate,  $T$  the workpiece temperature,  $T_r$  the reference temperature and  $T_m$  the melting temperature (Table 3).

The results of the 3D FEM simulation can be seen in Fig. 6. The data of the mechanical loads were averaged and validated with the experimentally measured values of feed force and drilling torque (Fig. 6a). On both, the feed force and the drilling torque the curves of the experiment show a plateau after an approximate time of  $t=5$  s, which means that the values do not increase any further. Therefore, the validation of the model takes place after this value in a time interval of  $t=0.0016$  s, which represents 0.75 tool revolutions. The values of the simulation in this time interval also form a plateau, therefore they represent the constant material

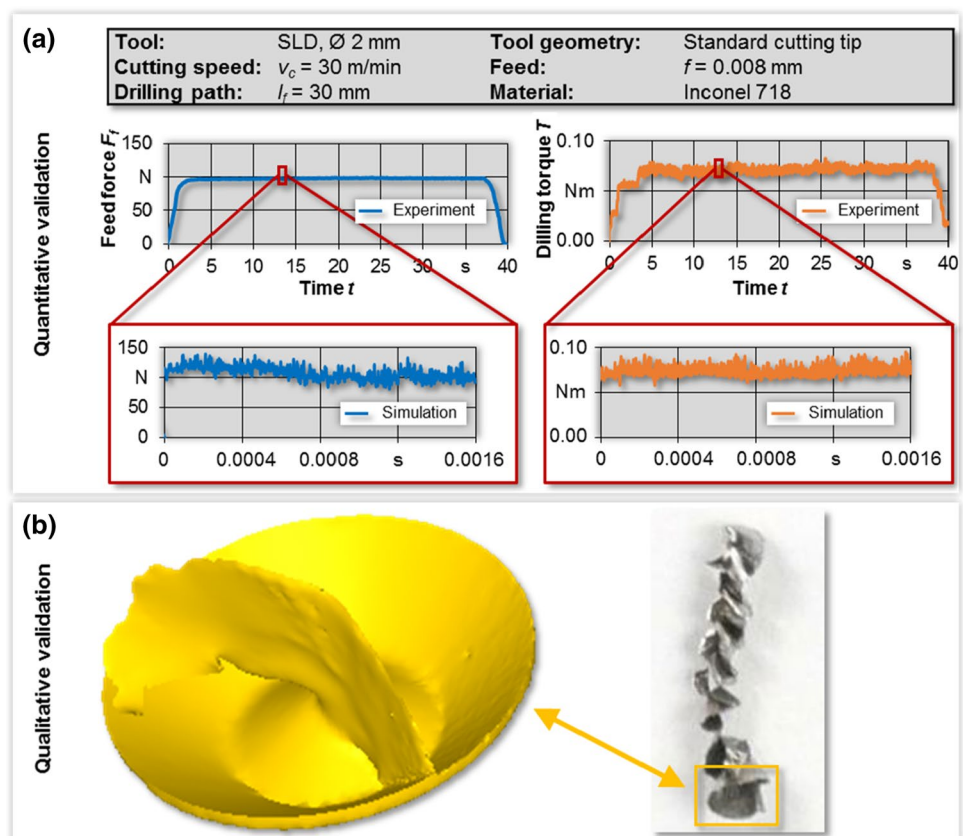
deformation and chip formation in the cutting zone. To reach this behavior it is important to have a cutting engagement similar to the chip formation process and a good contact of the tool model and the model of the bore hole bottom at the start of the simulation. The feed forces increase only slightly up to the complete engagement of the cutting edge and the beginning of the actual chip formation and reach their maximum load. The drilling torques behave similarly. In the comparison of the feed forces it can be seen that the experimentally measured feed forces with  $F_f=100$  N are lower than the numerical calculated feed forces of  $F_f=120$  N. One of the reasons is that the experimental results are influenced by a variety of factors such as the process specific machine requirements, the static and dynamic tool behavior and the coolant lubricant influence. The drilling torque from the simulation with  $T=0.9$  Nm is a little higher than the measurement data with  $T=0.8$  Nm. Overall, the results of the simulation show a very good agreement with the experimental data, so that a good model quality was achieved.

Figure 6b shows the result for the chip formation, which was validated qualitatively by comparing the small chip

**Table 3** Parameters for the Johnson & Cool material model [26]

A in MPa	B in MPa	n	C	$\dot{\epsilon}$ in 1/s	m	$T_r$ in K	$T_m$ in K
450	1700	0.65	0.017	0.001	1.3	293.15	1863.15

**Fig. 6** a Quantitative validation of the feed force and drilling torque. b Qualitative validation of the chip formation



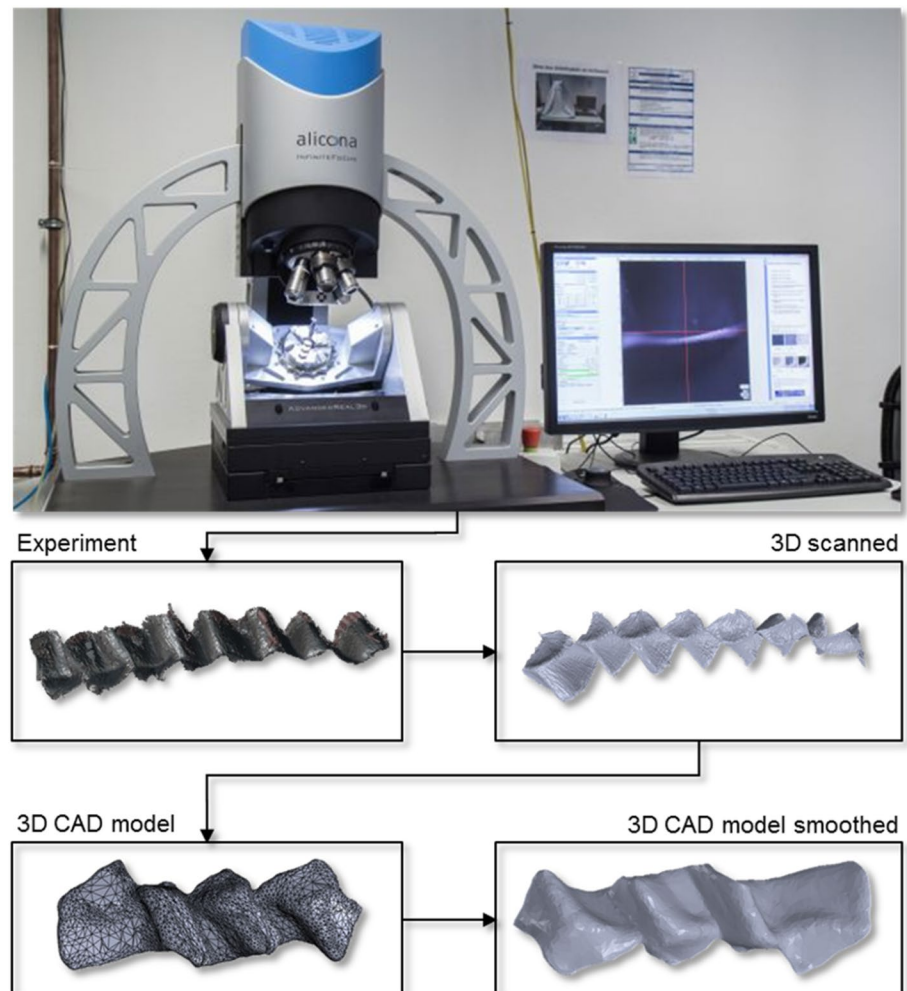
from the simulation to the first segment of a chip from the experiment. The chip from the experiment was analyzed with a microscope, type Keyence VHX-5000. In the first moment it is remarkable that the chip shape of the experiment shows a long and folded chip. The chip formation starts when the cutting edge of the tool comes into contact with the workpiece. During the micro single-lip deep hole drilling process the chip is formed along the inner and outer cutting edge in a direction perpendicular to the rake face. Since there is a difference in cutting speed along the cutting edge starting from  $v_c = 0$  m/min in the center of the bore hole to the nominal cutting speed of  $v_c = 30$  m/min at the corner of the cutting edge the chip curls up and collides with the tool and the bore hole bottom. It depends on the cutting edge design and the material behavior if a spiral chip is formed or if the chip is folded in an irregular shape. It can be seen that the simulated chip formation for the first section appears to be almost identical to the first section of the chip from the experiment. Therefore the FEM model was qualified for future innovative applications in which the behavior of the cooling lubricant will

be analyzed while considering the chip formation at the cutting edge and the chip transport through the chip flute.

#### 4 Geometrical representation of the chip

FEM simulations are a good tool to evaluate the chip formation and allows the prediction of the chip shape considering the factors of cutting parameters and material properties. However, for economic reasons it is not possible to simulate the complete chip formation process since for longer simulated chip length the time for numerical calculations increases enormously. In order to include a complete chip in further applications the geometric representation of a chip is modeled from the experiment. This geometric representation of the chip will be then positioned into the flute so that the coolant lubricant flow can be analyzed with a CFD simulation considering the chip formation and also the chip removal. The chip shape from the experiment is digitized with the optical 3D measurement system Alicona Infinite Focus G5 (Fig. 7).

**Fig. 7** Analysis of the chip shape and generation of the chip shape model





As noted above the result of the experiment are long and folded chips. The chips consist of individual segments which are curled up at the cutting edge, and folded between chip flute and the bore hole bottom during the chip removal process. It can be attributed to the mechanics of micro cutting and the material properties of Inconel 718 which hinder chip breakage and the formation of short chips. The chip shape itself is irregular and has a lot of micro burrs. This results in a high number of measurement points during the digitalization and also makes the scan of a closed geometric model very difficult. In the subsequent preparation of the measurement data from the 3D measurement system the burrs at the corners of the chips and the irregularities (holes) of the scan must be removed.

To use the geometric model of the chip in a CFD simulation of the coolant lubrication the number of measuring point must be reduced and the surface of the chip needs to be smoothed in order to minimize the necessary computing power to mesh the highly irregular surface of the chip for the fluid model. The data of the digitally scanned chip is therefore transferred into the software SolidWorks where a standard triangulation language (STL) file of the chip shape is generated. To smooth the surface the chip model is further processed with the open-source software MeshLab. This program is developed for processing three-dimensional unstructured meshes and recognizes the edges and nodes of the polygons. Non-referenced corner points are removed. The burrs on the chip leading to image noise are removed with a smoothing factor of 0.5. The modified chip shape model is transferred back into the CAD-software and positioned in the chip flute to check whether it is possible to generate a fluid model for the future consideration of the chip in fluid simulations of the coolant flow. Figure 8 shows the complete CAD model for the consideration of the chip formation and the chip removal in a CFD simulation of the cooling lubricant supply for further investigations of the single-lip deep hole drilling process.

## 5 Conclusions

In this article, the chip formation during micro single-lip deep hole drilling with a diameter of  $d=2$  mm at varying coolant pressures of  $p=80$  bar,  $p=100$  bar and  $p=120$  bar was investigated. In addition to the mechanical tool loads, feed force and drilling torque, the chip forms, the tool wear and the bore hole quality in the form of surface roughness as well as diameter and roundness deviations were evaluated. For a cutting speed of  $v_c=30$  m/min and a feed rate of  $f=0.008$  mm the drilling process is stable and leads to continuously rising tool wear without sudden tool failure. The coolant pressure shows only a small influence on mechanical loads and bore hole quality. A tendency to produce slightly

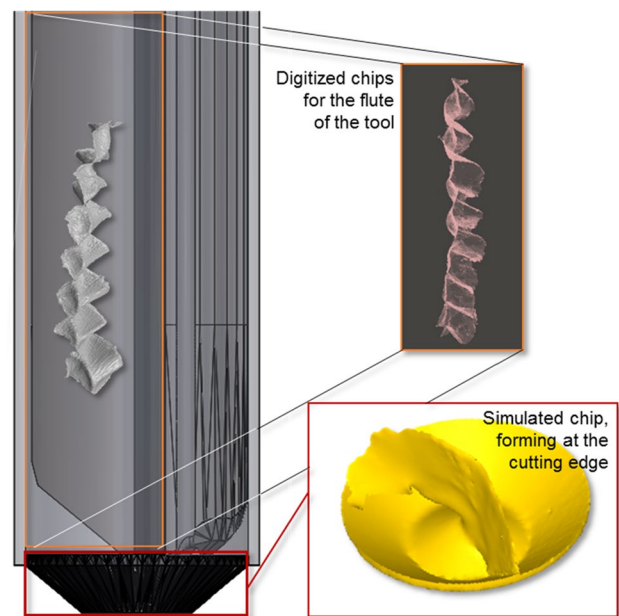


**Fig. 8** Position of the chip shape model in the chip flute and the chip formation model at the bore hole bottom

shorter chips for higher pressures was visible. The highest cooling lubricant pressure of  $p=120$  bar, however, shows an advantage in terms of tool wear. However, with the standard cutting tip geometry with angles of incidence of  $\kappa_1 = 50^\circ$  at the outer and  $\kappa_2 = 120^\circ$  at the inner cutting edge the process generates long and unfavorable chips which will lead to complications for higher feed rates and cutting speeds exceeding the tool stability and leading to tool failure. To increase the productivity of the drilling process and to optimize the drilling tool it is necessary to analyze the process comprehensively taking into account the interactions of tool geometry, chip formation, thermo-mechanical loads, chip transport and cooling lubricant supply.

In a first step to this comprehensive analysis a FEM model was generated based on the experimental data to simulate the chip formation in the software DEFORM 3D. The modeling of the micro dimensions and the meshing constitute major challenges, since the minimum element edge length of the grid must be three times smaller than the uncut chip thickness. Corresponding to the used feed rate of  $f=0.008$  mm this results in a very small value of  $le=0.0027$  mm. The results of the chip formation simulation were validated with the experimental data of feed force and drilling torque showing a good agreement between simulation and experiment. Additionally a qualitative validation of the chip formation was carried out, showing no differences for the first section of the emerging chip. In this context the 3D FEM model was qualified and will be used for the development of an advanced predictive performance model of the drilling process which considers also the behavior of the coolant lubricant in addition to the tool geometry and

the chip formation. However, as an innovative approach the chip removal will also be closely involved in the further investigations. Therefore, the chip shape of a complete chip must be included. Since due to the limited computational power a 3D FEM simulation of the chip shape is not possible a geometrical representation using a digital 3D scan was generated. For the new innovative approach the generated model will be post-processed and smoothed until it is possible to generate a fluid model. The presented modeling of the drilling process is a very important basis for the development of the comprehensive simulation model, which will take the chip formation and the chip removal through the chip flute into account during the analysis of the coolant flow. Especially in machining technology it is necessary to understand the interactions between fluid / tool / workpiece / chip formation / chip shape and chip removal to optimize tool geometries and process parameters. Therefore, only with a deeper insight and knowledge of the micro single-lip deep hole drilling process as a whole it will be possible to improve productivity. Simulations of the process moreover help to reduce the development costs by minimizing the number of necessary experiments to evaluate different cutting parameters, tool geometries as well as the cooling lubricant strategies. With the investigations presented here, a validated model basis was created, which is expandable and allows a deeper process understanding of the micro single-lip deep hole drilling process of difficult-to-machine materials.

**Acknowledgements** The authors gratefully acknowledge funding from the German Research Foundation (DFG) for the research project (405605200).

**Author contributions** All authors contributed to the conception and design of the study and read and approved the final manuscript.

**Funding** German Research Foundation (DFG) (405605200).

**Data availability** Not applicable.

## Compliance with ethical standards

**Conflicts of interest** The authors declare that they have no conflict of interest.

**Ethical approval** Not applicable.

**Consent to participate** Not applicable.

**Consent to publish** The authors agree to publication this paper.

## References

- Xavier L, Elangovan D (2013) Effective parameters for improving deep hole drilling process by conventional method—a review. *Int J Eng Res Technol* 2
- Malarvizhi S, Chaudhari A, Woon KS, Kumar AS, Rahman M (2016) Influence of burnishing axial interference on hole surface quality in deep hole drilling of inconel 718. *ProcManuf* 5:1295–1307. <https://doi.org/10.1016/j.promfg.2016.08.101>
- Bleicher F, Reiter M, Brier J (2019) Increase of chip removal rate in single-lip deep hole drilling at small diameters by low-frequency vibration support. *CIRP Ann-Manuf Tech* 68:93–96. <https://doi.org/10.1016/j.cirp.2019.04.028>
- Biermann D, Bleicher F, Heisel U, Klocke F, Möhring HC (2018) Deep hole drilling. *CIRP Ann-Manuf Tech* 67:673–694. <https://doi.org/10.1016/j.cirp.2018.05.007>
- Reiter M, Bleicher F (2019) Affection of chip formation in single-lip deep hole drilling at small diameters by application of low-frequency vibration support. *MM SJ* 2019:3107–3113. [https://doi.org/https://doi.org/10.17973/MMSJ.2019\\_11\\_2019058](https://doi.org/https://doi.org/10.17973/MMSJ.2019_11_2019058)
- Biermann D, Heilmann M (2011) Hybrid Manufacturing of Deep Holes With Small Diameters. In: *Proceedings of the ASME International Manufacturing Science and Engineering Conference: Presented at ASME 2011 International Manufacturing Science and Engineering Conference*, June 13–17, 2011, Corvallis, Oregon, USA. American Society of Mechanical Engineers, New York, N.Y., pp 417–425
- Zhou J, Bushlya V, Avdovic P, Stahl JE (2012) Study of surface quality in high speed turning of Inconel 718 with uncoated and coated CBN tools. *Int J AdvManufTechnol* 58:141–151. <https://doi.org/10.1007/s00170-011-3374-7>
- Dudzinski D, Devillez A, Moufki A, Larrouquere D, Zerrouki V, Vigneau J (2004) A review of developments towards dry and high speed machining of Inconel 718 alloy. *Int J Mach Tools Manu* 44:439–456. [https://doi.org/10.1016/S0890-6955\(03\)00159-7](https://doi.org/10.1016/S0890-6955(03)00159-7)
- Biermann D, Kirschner M (2015) Experimental investigations on single-lip deep hole drilling of superalloy Inconel 718 with small diameters. *J Manuf Processes* 20:332–339. <https://doi.org/10.1016/j.jmapro.2015.06.001>
- Chaudhari A (2016) A study on straightness control in deep hole drilling of Inconel 718. Dissertation, National University of Singapore
- Chen YC, Liao YS (2003) Study on wear mechanisms in drilling of Inconel 718 superalloy. *J Mater ProcessTech* 140:269–273. [https://doi.org/10.1016/S0924-0136\(03\)00792-1](https://doi.org/10.1016/S0924-0136(03)00792-1)
- Sharman ARC, Amarasinghe A, Ridgway K (2008) Tool life and surface integrity aspects when drilling and hole making in Inconel 718. *J Mater Process Tech* 200:424–432. <https://doi.org/10.1016/j.jmatprotec.2007.08.080>
- Jawahir IS, van Luttervelt CA (1993) Recent developments in chip control research and applications. *CIRP Ann-Manuf Tech* 42:659–693. [https://doi.org/10.1016/S0007-8506\(07\)62531-1](https://doi.org/10.1016/S0007-8506(07)62531-1)
- Luttervelt CA, Childs THC, Jawahir IS, Klocke F, Venuvinod P, Altintas Y, Armarego E, Dornfeld D, Grabec I, Leopold J, Lindstrom B, Lucca D, Obikawa T, Shirakashi D, Sato H (1998) Present situation and future trends in modelling of machining operations progress report of the CIRP working group ‘modelling of machining operations.’ *CIRP Ann-Manuf* 47:587–626. [https://doi.org/10.1016/S0007-8506\(07\)63244-2](https://doi.org/10.1016/S0007-8506(07)63244-2)
- Arrazola PJ, Özel T, Umbrello D, Davies M, Jawahir IS (2013) Recent advances in modelling of metal machining processes. *CIRP Ann-Manuf Technology* 62:695–718. <https://doi.org/10.1016/j.cirp.2013.05.006>
- Ehmann KF, Kapoor SG, DeVor RE, Lazoglu L (1997) Machining process modeling: a review. *J ManufSciEng* 119:655–663. <https://doi.org/10.1115/1.2836805>
- Mackerle J (1999) Finite-element analysis and simulation of machining: a bibliography (1976–1996). *J Materials Process Technol* 86:17–44. [https://doi.org/10.1016/S0924-0136\(98\)00227-1](https://doi.org/10.1016/S0924-0136(98)00227-1)

18. Mackerle J (2003) Finite element analysis and simulation of machining: an addendum A bibliography (1996–2002). *Int J Mach Tools Manu* 43:103–114. [https://doi.org/10.1016/S0890-6955\(02\)00162-1](https://doi.org/10.1016/S0890-6955(02)00162-1)
19. Soo SL, Aspinwall DK, Dewes RC (2004) 3D FE modelling of the cutting of Inconel 718. *J Mater Process Tech* 150:116–123. <https://doi.org/10.1016/j.jmatprotec.2004.01.046>
20. Abouridouane M, Klocke F, Lung D (2013) Microstructure-based 3D finite element model for micro drilling carbon steels. *Proc CIRP* 8:94–99. <https://doi.org/10.1016/j.procir.2013.06.071>
21. Chaudhari A, Malarvizhi S, Woon KS, Kumar AS, Rahman M (2015) The effects of pilot hole geometry on tool-work engagement efficacy in deep hole drilling. *J Manuf Process* 19:135–141. <https://doi.org/10.1016/j.jmapro.2015.06.006>
22. Brinksmeier E, Meyer D, Huesmann-Cordes AG, Herrmann C (2015) Metalworking fluids-Mechanisms and performance. *CIRP Ann-Manuf Tech* 64:605–628. <https://doi.org/10.1016/j.cirp.2015.05.003>
23. Hexagon MSC Software (2013) The Best FEA Mesh Density for Accuracy and Speed | MSC Nastran. <https://simulatemore.mscoftware.com/the-best-fea-mesh-density-for-accuracy-and-speed-msc-nastran/>. Accessed 13 Nov 2020
24. Uçak N, Çiçek A, Oezkaya E et al (2019) Finite element simulations of cutting force, torque, and temperature in drilling of Inconel 718. *Proc CIRP* 82:47–52. <https://doi.org/10.1016/j.procir.2019.03.277>
25. Johnson GR, Cook WH (1983) A constitutive model and data for metals subjected to large strains, high strain rates and high temperatures. *Proceedings of the 7th Symposium on Ballistics, The Hague*: 541–547
26. Baohai W, Di C, Xiaodong H, Dinghua Z, Kai T (2016) Cutting tool temperature prediction method using analytical model for end milling. *Chin J Aeronaut* 29:1788–1794. <https://doi.org/10.1016/j.cja.2016.03.011>

**Publisher's Note** Springer Nature remains neutral with regard to jurisdictional claims in published maps and institutional affiliations.